Influence of Internal Climate Variability on Estuarine Sediment Dynamics

S. Dietrich & A. Winterscheid
Federal Institute of Hydrology, Koblenz, Germany

ABSTRACT: Climate variability influences the sediment yield in North Sea estuaries such as the Elbe River Estuary. A clear task for the improvement of sediment management is to evaluate the basic influences between climate, the hydrological regime and estuarine sediments dynamics. Especially long-lasting low discharge events highly affect the transport of suspended sediment stream upwards the estuary due to the intensification of tidal pumping. Climate dynamical interpretations are especially important for an enhanced understanding of estuarine sediment dynamics.

For this study we investigate the daily Elbe freshwater discharge at the station Neu-Darchau for the years 1902-2013. We perform a hierarchical cluster analyses to group the discharge of the single water years into typical discharge modes. These clusters show distinct interannual to multidecadal variability. We analyse these clusters to evaluate the relationship with large-scale climatic conditions such as sea surface temperatures (HadISST1) as well as the general atmospheric circulation patterns based on Hadley Centre's sea level pressure (HadSLP2).

The cluster analysis results in five different clusters demonstrating typical modes of freshwater discharge. These clusters can be associated with global modes of internal climate variability as well as of global warming. Internal climate variability on interannual like the North Atlantic Oscillation (NAO) or the El Niño Souther oscillation (ENSO), over decadal fluctuation like the Pacific Decadal Oscillation (PDO) through multidecadal variability such as the Atlantic Multidecadal Oscillation (AMO) have been found to be an important driving force in the calculated discharge clusters. Climate dynamical interpretations are therefore important for an enhanced understanding of estuarine sediment dynamics and might be thus usable as a improved tool for future sediment management issues.

Keywords: Internal climate variability, Freshwater discharge, Sediment transport, Estuary

1 INTRODUCTION

Climate variability influences the hydrology and thus the sediment yield in North Sea estuaries such as the Elbe River Estuary (Fig. 1). The maintenance of the navigable water depths in the estuaries is strongly influenced by freshwater discharge and requires dredging and disposal of large amounts of sediments. Especially those periods of persistent low freshwater discharge (hereinafter referred to as discharge only) lasting for several weeks or month highly affect the transport of suspended sediment stream upwards the estuary due to enhanced tidal pumping. On the other side enhances high river runoff the natural output of fine sediment from the estuary towards the German Bight, thus it supports the dredging and sediment management in safeguarding the required output rate (BfG, 2014).

To evaluate the link between climate forcing and hydrology that drives sediment transport it is necessary to study the hydrological variability on climate time scales. Evidence from long lasting hydrological records demonstrates a linkage between persistent climate anomalies and anomalous hydrological behaviour (Arnell, 1992). These anomalies often have its origin in internal modes of climate variability that are represented as global teleconnetion pattern that affect European climate commonly referred to Hurrell (1995), Wallace and Gutzler (1981), Barnston and Livezey (1987), or Mantua et al. (1997). All these pat-

terns also interference with each other and are well known to exert a strong influence on on European climate (Comas-Bru and McDermott, 2014).

Figure. 1. Map of Elbe catchment area. The gauge station at Neu Darchau is marked.

Here, the two most important global teleconnections that influence European river discharge variability are the North Atlantic Oscillation (NAO) and the El Niño-Southern Oscillation (ENSO), respectively (Cullen et al., 2002; Dettinger and Diaz, 2000). However, the third big driver manipulating river discharge are the sea surface temperatures (Ionita et al., 2011; Rimbu et al., 2005).

The most prominent example of large-scale teleconnections patterns of extra-tropical atmospheric circulation variability is the NAO (Hurrell, 1995) and the related Arctic Oscillation (AO, Zhou et al., 2001), also called Northern Annular Mode (NAM). The AO/NAO is the leading mode of climate variability in the North Atlantic region and is characterized by a typical meridional dipole anomaly of sea level pressure (SLP). This SLP oscillation is accompanied by changes in wind, air temperature, and humidity transport across the North Atlanitic and Europe and is associated with a typical tripolar SST pattern over the North Atlantic. The positive mode of the NAO is associated with a cold anomaly in the subpolar region, a warm anomaly in the middle latitudes, and a cold subtropical anomaly between 30°N and the equator (vice versa during the negative NAO). Also the AO/NAOis most prominent during the boreal winter, the summer NAO (SNAO) exerts a strong influence on European climate as well through changes of the position of the North Atlantic storm track: During the positive phase of the SNAO Northwest Europe experience significantly reduced cloudiness with anomalous warm temperatures, while over the eastern Mediterranean cloudiness increases (Folland et al., 2009). Correlation of the NAO index with hydrological data have show a correspondence between NAO controlled precipitation anomalies and river flow: a high (low) NAO index leads to an increased (decreased) river discharge in northern Europe and a vice versa behaviour in southern Europe (e.g. Dettinger and Diaz, 2000).

The large-scale organization of SST patterns is mainly influenced by large-scale anomalies of the atmospheric circulation and attendant changes in the turbulent and radiative energy fluxes at the air-sea interface and local wind-driven Ekmann currents (Deser et al., 2010 and references therein). However, the oceans play a major role due to their large heat-storage capacity: Approximately 3.5 m of water contains as much energy as the whole atmosphere.

The global leading mode of monthly SST anomalies is the ENSO. The ENSO-related spatial SST pattern of its warm phase acrosses the eastern two thirds of the tropical Pacific and is flanked by weaker negative anomalies from the north over the far western to the South Pacific. ENSO related SST anomalies also occur over the North Atlantic as well. The atmosphere acts here as a bridge: The wintertime ENSO generates over the North Atlantic a NAO-like SLP dipole with a subsequent SST response during spring (Deser et al., 2010). However, while the NAO-like SLP pattern more correspond to the positive phase of the NAO the generated SST pattern is more similar to the pattern that is associated to the negative NAO. In addition suggest observations and modelling studies that the ENSO teleconnection is more robust during La Niña compared with El Niño events (Pozo-Vázquez et al., 2001).
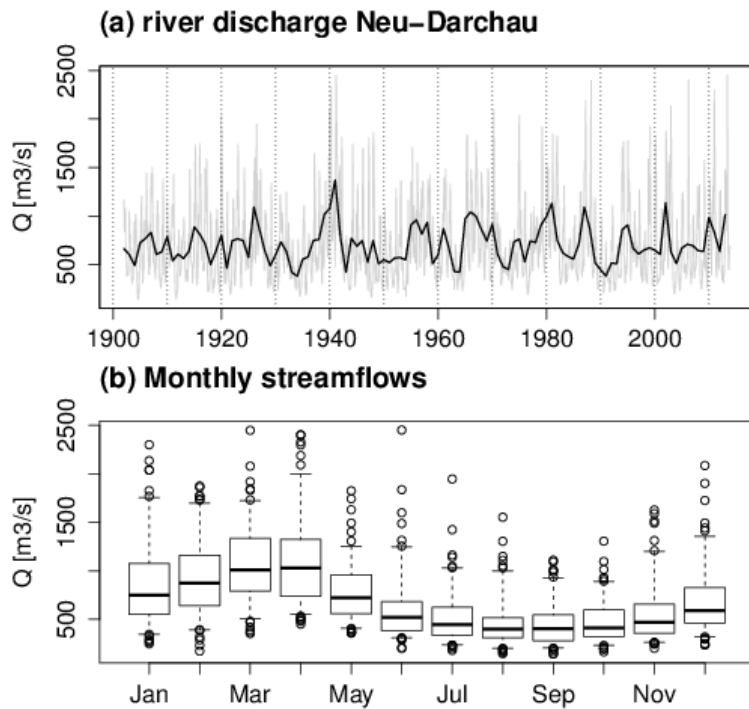
Figure 2. River discharge of Elbe River at gauge Neu Darchau. (a) annual (black) and monthly (light grey) mean values, (b) seasonal cycle. The whiskers of the boxplots show the 10% or 90% percentile, respectively. The bold black bars show median values, circles show ourliers. The river discharge is characterizes by strong interannual to decadal variability (a). The seasonal signal shows highest

The leading mode of monthly SST anomalies over the North Pacific exhibits considerable decadal variability and is called the Pacific Decadal Oscillation (Mantua et al., 1997). The spatial pattern of PDO associated SST anomalies is similar to ENSO, however, the relative weighting between the north and the south Pacific is different: While during ENSO the South Pacific exhibits the strongest magnitude, during the PDO this is true for the North Pacific (Mantua and Hare, 2002).

The influence of these parameters on runoff of European rivers have already been demonstrated by several studies for interannual to multidecadal changes (Ionita et al., 2008, 2011; Rimbu et al., 2005) as well as for extreme events such as flash floods (Petrow and Merz, 2009). However, this paper focus on two main questions: (1) How often does occur specific discharge conditions of the Elbe River. In the case of estuarine sediment management we are especially interested in the frequency and seasonality of persistent low discharge conditions? (2) How are these specific run-off conditions related to internal modes of climate variability expressed by sea level pressure (SLP) and sea surface temperature (SST) fields?

2 DATA AND METHODS

The Elbe River is one of the largest rivers in Europe and especially the Elbe River Estuary is of major importance for transportation with commercial navigation vessels towards the Port of Hamburg (Germany). The Elbe rises in the Giant mountains in the Czech Republic and discharges into the German Bight, North Sea. It is approximately 1,100 km long and covers a catchment area of about 150,000 km² (Fig. 1). For this study we investigate the daily Elbe discharge at the station Neu-Darchau (53° 14′ N, 10° 53′ E) for the years 1902-2013 (data origin: http://coast.gkss.de/staff/kappenberg/runoff_data/elbe.abfluss). Neu Darchau is the last gauging station in the lower part of the Elbe River upstream of the weir in Geesthaacht and is therefore not influenced by tidal dynamics.

The mean discharge of the Elbe River is approximately 700 m³/s and has a pronounced seasonal cycle with maximum stream flow during spring and minimum values during late summer and autumn (Fig. 2a). This pattern is according to the definition of the hydrological year (also discharge year) that covers a period of 12 months and accounts for the annual budget of meteoric precipitation that is fallen as ice or snow and is therefore storaged within the catchment influencing the discharge of the subsequent year. The discharge year begins in November by definition and is characterized by increasing values until peak values in April, dominated by winter precipitation and snow melt, and subsequent declining values. In addition, the 110 year-long time series for discharge shows a distinct interannual to decadal variability (Fig. 2b).

We perform a hierarchical cluster analyses to group the discharge of the single hydrological years into typical discharge modes. Subsequently, we analyse these clusters to evaluate the relationship with synoptic weather patterns to foster a climate dynamical interpretation. Here, we study sea surface temperatures (SST), sea ice (SIC) as well as the general atmospheric circulation patterns (SLP) based on Hadley Centre's sea level pressure (HadSLP2, Allan and Ansell, 2006) and the combined sea surface temperatures and sea ice datasets (HadISST1, Rayner et al., 2003), which cover the period of our freshwater discharge time series.

2.1   Cluster Analysis

The cluster analysis is applied to detect common patterns in the 110 realizations of hydrological years (1902-2013). A outlier detection prior to the cluster analysis was not applied, because extreme events are also in the focus of this study. The discharge data are smoothed with a 14-day running mean filter to remove the high-frequency signal within the data and to obtain persistent periods with similar discharge.

The hierarchical cluster analysis uses the "Manhattan" (also city-block) method when computing the distance matrix between two observation (Mardia et al., 1979): The Manhattan method calculates the absolute distance between two vectors. In comparison to the euclidean distance measure distant objects (like outliers) are much less weighted. This distance matrix is used for subsequent hierarchical clustering. At each stage distances between clusters are recomputed by the Lance–Williams dissimilarity update formula according to the particular clustering method being used. For the analysis the Ward's minimum variance method has been chosen. The aim of the Ward method is the union of those objects that lead to the lowest increase of the cluster's distribution width. The result is a tree that describes the similarities of the different hydrological years (not shown). This tree is subsequently cut into five groups. This number has been chosen according to expert judgement, because the number of five is according to the number of atmospheric and oceanic teleconnection patterns as well as global warming trends that might influence the Elbe discharge on interannual to decadal timescales.

2.2   Composite Maps

For each of the five clusters composites of major climate variables are calculated. In this context we analyse the correspondence of our clusters to large-scale climatic conditions such as sea surface temperatures, sea ice as well as the general atmospheric circulation patterns based on Hadley Centre's sea level pressure (HadSLP2; Allan and Ansell, 2006) and sea surface temperature datasets (HadISST1; Rayner, 2003), which cover the period of our freshwater discharge time series. The gridded HadSLP2 dataset was created using marine observations taken from ICOADS and land (terrestrial and island) observations from 2228 stations around the globe and has a resolution of 5° x 5°. The HadISST data has a resolution of 1° x 1°. The results are plotted as anomalies to visualize the change versus the long-term mean (1902-2013).

3 RELATION OF ELBE DISCHARGE WITH GLOBAL TELECONNECTION PATTERNS

In this section we analyse the relation between the freshwater discharge (gauging station Neu Darchau) with global SLP and SST data. Here, we evaluate the climatic influence on different typical modes of annual discharge events. These modes are derived via cluster analysis of the14 d-smoothed daily discharge time series that results in five cluster with pronounced specific patterns (Fig. 3).

Cluster 1 hold the largest amount of members: 42 out of 110 investigated hydrological years belong to cluster 1 (38.2%). It is characterized by the lowest discharge values and the mean values of this cluster follow the mean monthly discharge shown in (Fig. 2b). This explains why this cluster is the most common one. However, two outliers occur in April (1943) and in July (1952), respectively.

Cluster 2 (23.6% of the discharge years) is characterized by much higher discharge values. The maximum mean discharge during spring reaches 1,500 m³/s. Some discharge years in cluster 2 also show a second peak during summer that has, however, no significant influence on the cluster mean value. Beside an overall higher level of discharge the shape of cluster 2 is similar to that one of cluster 1.
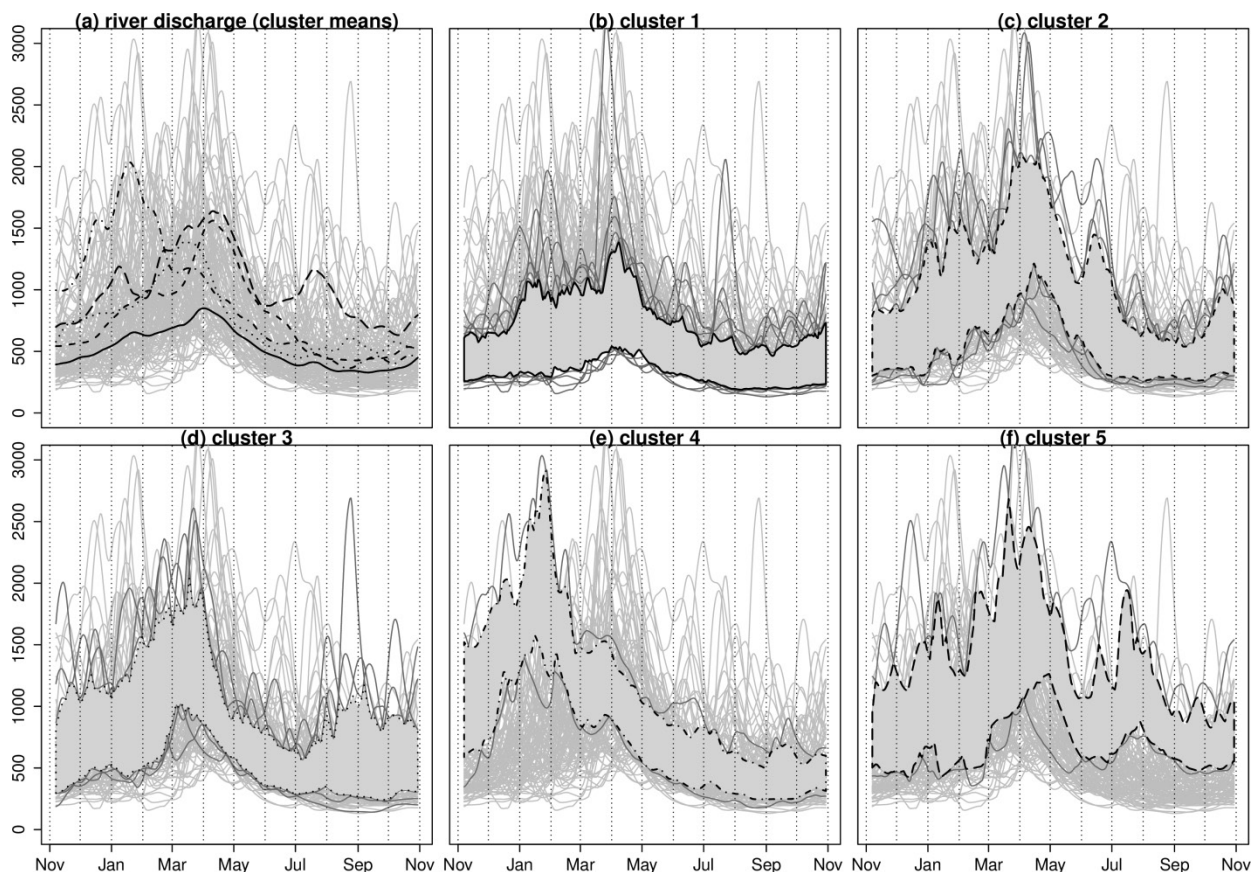
Figure 3. Seasonal freshwater discharge cycls (m³/s) of clusters following the hydrological year starting in November. Light gray curves show all single realizations of the discharge years between 1902 and 2013. (a) represents the cluster mean values, the line type corresponds to the borderline of the patches given in (b-f). Gray patches with the specific bold border shows the 10%-90% percentiles values. Dark gray curves represent the members of the given cluster. All curves are basing on daily values, smoothed with a 14-day running mean filter.

Cluster 3 (21.8%) shows similar runoff characteristics like cluster 2. However, the discharge peak occurs one month earlier in March. In addition, the variability of river flow starts to increase after August.

This trend is continued by cluster 4 (7.3%), which is characterized by an extremly high discharge early in the year during January. The mean discharge of cluster 4 exceeds 2,000 m³/s and declines to quite low levels similar to cluster 1 later in the year.

Cluster 5 (9.1%) represents high discharge not only during the spring snow melt. Over the whole year the runoff is strongly increased and reaches remarkable levels also during summer and autumn. In addition, around August occur a secondary peak in this cluster that can also be seen in the cluster mean values.

The cluster analysis also answers the question after the seasonality of persistent low discharge conditions. Cluster 1 is of course the most prominent one that contains a high probability for periods of persistent low discharge (excluding the spring discharge). Cluster 2 demonstrates a good chance between mid of July and end of October, cluster 3 between May and August (later on the variability increases again). Cluster 4 shows after cluster 1 the second highest chance for periods of persistent low discharge events. The season starts in May and lasts until December. Finally, cluster 5 has been found to represent hydrological wet years. Thus, is is rather unlikely that low discharge events, especially persistent ones, occur.

To identify the characteristic forcing of each clusters (question 2) we calculated for each cluster composite maps for SLP (not shown) and SST (Fig. 4), which are represented as anomalies against the long-term mean from 1902-2013. The composites from cluster 1 and cluster 2 show only weak signals. However, even here SST patterns that correspond to global teleconnection patterns are visible.

Cluster 1 can be associated with a weak positive NAO signal, with its tripolar SST pattern (cold at the Labrador Sea, slight warming at the North Atlantic current, and cold temperatures again at low latitudes). In addition, there is also a weak trend towards the positive phase of the PDO visible.
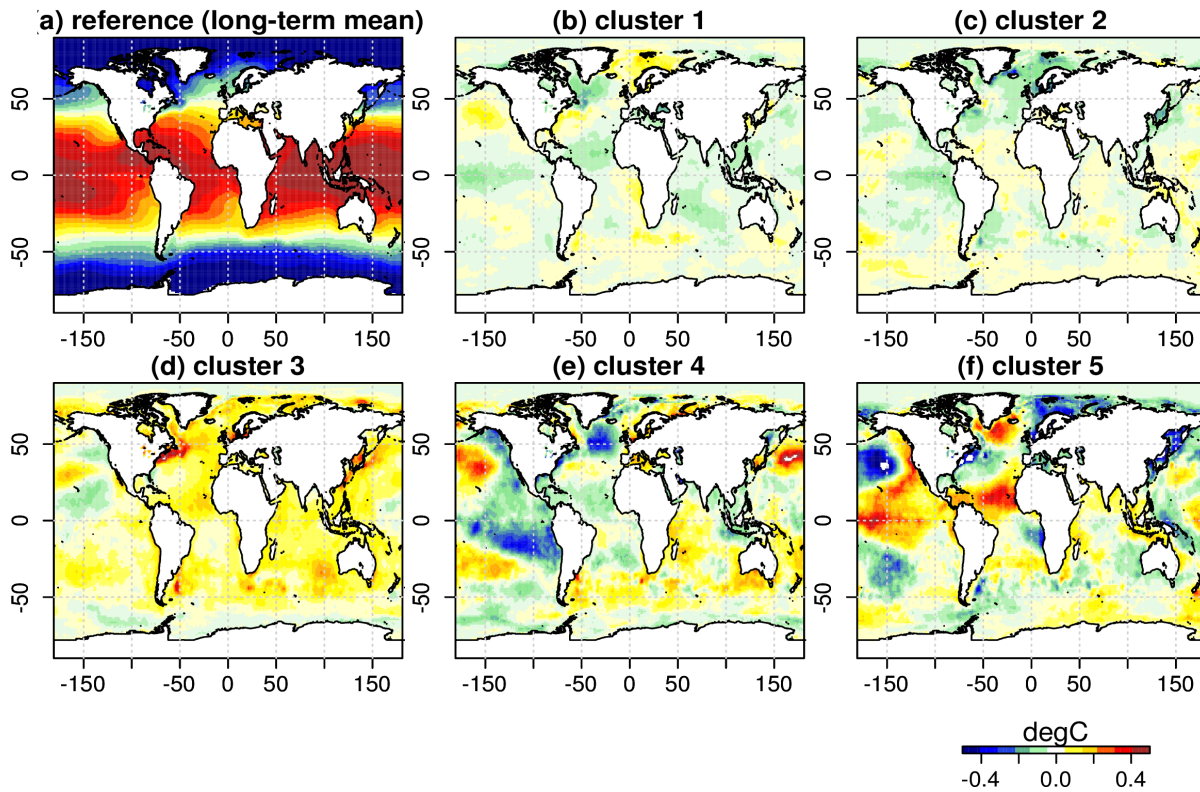
sst composite maps (hyrol. year)

Figure 4. HadISST sea surface temperature maps: (a) long-term mean (1902-2013), (b-f) composite maps (plotted as anomalies of the long-term mean) of the single clusters.

Cluster 2 is marked by a weak signal of a negative PDO as well as bipolar cooling at the North Atlantic related to slight warming of the tropical Atlantic.

Cluster 3 shows a clear signal of global warming that affects both the North and the South hemisphere. Strongest SST warming occur at the western branch of the North Atlantic current and the Labrador region as well as in the North Sea. While the Pacific tends to be also influenced by a negative PDO pattern, the rest of the Earth's oceans shows a warming pattern.

Clusters 4 and 5 show the strongest signals since their seasonal patterns represent the largest dissimilarities in comparison to the long-term mean. The most conspicuous feature is the clear anti-phase behaviour between both clusters. While cluster 4 is dominated by a clear negative PDO in combination with a typical positive NAO pattern, cluster 5 shows the opposite trends: a pronounced positive PDO and a pronounced negative NAO SST pattern, respectively. This phase shift is also demonstrated in the corresponding SLP values also indicating a dominant influence of teleconnections (not shown). In addition, cluster 5 corresponds to the late phase of global ENSO teleconnections via the atmospheric bridge (Deser et al., 2010).

4 DISCUSSION AND CONCLUSIONS

In this study we investigated common modes of the Elbe discharge at the gauging station Neu Darchau and their connection with large-scale teleconnection patterns based on SST (and SLP) data. In addition, we analysed clusters of the annual discharge hydrograph in order to estimate the occurrence of persisting low and high discharge events. The regime of the freshwater discharge, in particular periods of persistent low discharge, has a strong influence on turbidity. A persistent low discharge intensifies the tidal pumping effect, which leads to an accumulation of large amounts of SPM in the upper part of the River Elbe Estuary (Winterscheid et al., this issue).

The likeliness of periods of persisting low discharge is highest during summer and autumn. Especially clusters 1 and 4 are characterised by such low discharge during summer and autumn. Limited correspondence is further observable in cluster 2 (high number of periods with persistent low discharge in late autumn) and cluster 3 (low discharge during summer). Beside cluster 5 that is characterized by significantly increased discharge almost the whole of the hydrological year, all other clusters at least show, that periods of persistent low discharge can occur.
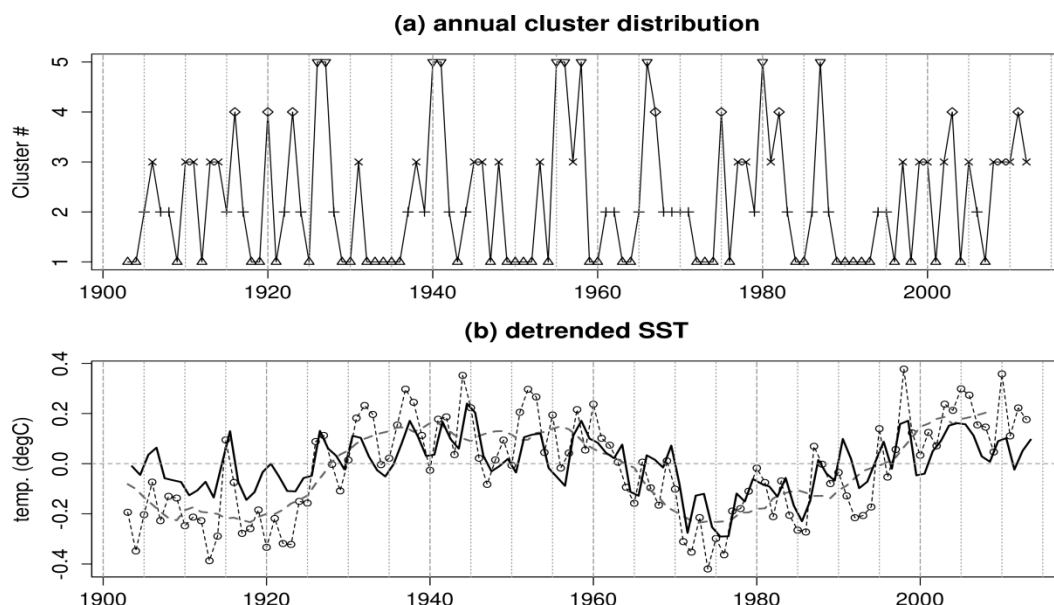
Figure 5. Time series of cluster analysis (a) in comparison to detrended sea surface temperatures (b): annual mean (dashed line) and 11-year running mean AMO index (bold dashed line) as well as annual mean and detrended mean SST values (HadISST) from the whole northern hemisphere (bold line).

High discharge events are pronounced in clusters 2 to 5, respectively, with annual maximum discharge around April to May. Clusters 1 and 2 (both together account for nearly 2/3 of all cases) show a signal that is in correspondence to the mean monthly discharge (Fig. 2). The composite maps also show only weak anomalies in comparison to the long-term mean. However, cluster 1 slightly corresponds to the positive mode of the NAO, which strengthend meridional pressure gradient shifts the jet stream northwards (Hurrell, 1995). Thus, the Elbe catchment is likely to obtain less precipitation in comparison to cluster 2.

Cluster 4 and 5 are less common (16.4% of 110 investigated years). However, both represents the extremes. In cluster 4 the annual maximum discharge shows quite high values but breaks down after February. Here, the Pacific shows the strongest signal. This is similar to cluster 5, which is a collection of most of the extremely wet with a high discharge. Both clusters show SST patterns similar to that characterizing a negative (cluster 4) or the positive mode (cluster 5) of the PDO. Furthermore, cluster 5 shows a pronounced negative NAO SST pattern. Merkel and Latif (2002) suggest that an El Niño or a positive mode of the PDO weakens the North Atlantic meridional pressure gradient and shifts the North Atlantic storm tracks further south inducing wetter conditions over central Europe and thus in the Elbe catchment.

The mean hydrograph of cluster 3 is quite similar to cluster 1 and 2. However, its annual maximum is slightly shifted earlier the year and the variability in discharge increases during the autumn and early winter. The composite map for cluster 3 shows an global warming pattern. In similarity to the Elbe discharge time series also the clusters are characterized by an interannual to multidecadal variability (Fig. 5). Decadal oscillation oft the Elbe discharge is driven by climate interaction of nearly global scale (Ionita et al., 2011). Most of the cluster 3 cases fall into periods of increased SSTs, that are controlled by internal climate processes like the Atlantic Multidecadal Oscillation (AMO, Enfield et al., 2001). In addition, especially the last decade is also strongly characterized by cluster 3 events which is associated with the warmest decade ever measured in observational records of the Earth (IPCC 2013).

Effects of future global warming on regional hydrology of the Elbe catchment are also assessable: Global warming will especially effect high northern latitude winter temperatures. It is suggested that this will lead to a northerly shift if the sea ice edge and thus subsequently to an increase of blocking highs over Siberia and Scandinavia which transports cold and dry air masses towards (Deser et al., 2010; Screen and Simmonds, 2010). This mechanism is also consistent with the results from the KLIWAS ensemble project (Imbery et al., 2013) which demonstrates a decrease of winter discharge during winter (Nilson et al., 2014). This scenario is suggested to lead to anomalous low freshwater discharge in the Elbe River and thus to an intensification of the upstream transported fine sediment in the Elbe River Estuary (tidal pumping). This is also in agreement to cluster 3 when the winter/spring high discharge season is significantly shorter in comparison to all other scenarios (Fig. 3).

In summary, freshwater discharge is influenced by numerous global teleconnection patterns of internal climate variability acting on interannual to multidecadal time scales. Climate dynamical interpretations are therefore important for an enhanced understanding of estuarine sediment dynamics and might be thus usable as a improved tool for future sediment management issues.

REFERENCES

Allan, R., and Ansell, T. (2006). A new globally complete monthly historical gridded mean sea level pressure dataset (HadSLP2): 1850-2004. J. Clim. *19*, 5816–5842.

Arnell, N.W. (1992). Factors controlling the effects of climate change on river flow regimes in a humid temperate environment. J. Hydrol. *132*, 321–342.

Barnston, A.G., and Livezey, R.E. (1987). Classification, seasonality and persistence of low-frequency atmospheric circulation patterns. Mon. Weather Rev. *115*, 1083–1126.

BfG (2014). Sedimentmanagement Tideelbe - Strategien und Potenziale - Systemstudie II. Ökologische Auswirkungen der Unterbringung von Feinmaterial (Koblenz: Bundesanstalt für Gewässerkunde).

Comas-Bru, L., and McDermott, F. (2014). Impacts of the EA and SCA patterns on the European twentieth century NAO–winter climate relationship. Q. J. R. Meteorol. Soc. *140*, 354–363.

Cullen, H.M., Kaplan, A., and Arkin, P.A. (2002). Impact of the North Atlantic Oscillation on Middle Eastern climate and streamflow. Clim. Change *55*, 315–338.

Deser, C., Alexander, M.A., Xie, S.-P., and Phillips, A.S. (2010). Sea Surface Temperature Variability: Patterns and Mechanisms. Annu. Rev. Mar. Sci. *2*, 115–143.

Dettinger, M., D., and Diaz, H., F. (2000). Global Characteristics of Stream Flow Seasonality and Variability. J. Hydrometeorol. *1*, 289–310.

Enfield, D.B., Mestas-Nuñez, A.M., and Trimble, P.J. (2001). The Atlantic multidecadal oscillation and its relation to rainfall and river flows in the continental US. Geophys. Res. Lett. *28*, 2077–2080.

Folland, C.K., Knight, J., Linderholm, H.W., Fereday, D., Ineson, S., and Hurrell, J.W. (2009). The Summer North Atlantic Oscillation: Past, Present, and Future. J. Clim. *22*, 1082–1103.

Hurrell, J.W. (1995). Decadal Trends in the North Atlantic Oscillation: Regional Temperatures and Precipitation. Science *269*, 676–679.

Imbery, F., Plagemann, S., and Namyslo, J. (2013). Processing and analysing an ensemble of climate projections for the joint research project KLIWAS. Adv. Sci. Res. *10*, 91–98.

Ionita, M., Lohmann, G., and Rimbu, N. (2008). Prediction of Spring Elbe Discharge Based on Stable Teleconnections with Winter Global Temperature and Precipitation. J. Clim. *21*, 6215–6226.

Ionita, M., Rimbu, N., and Lohmann, G. (2011). Decadal variability of the Elbe River streamflow. Int. J. Climatol. *31*, 22–30.

IPCC (2013). Climate change 2013: The physical science basis (Cambridge, United Kingdom and New York, NY, USA: Cambridge University Press).

Mantua, N.J., and Hare, S.R. (2002). The Pacific decadal oscillation. J. Oceanogr. *58*, 35–44.

Mantua, N.J., Hare, S.R., Zhang, Y., Wallace, J.M., and Francis, R.C. (1997). A Pacific interdecadal climate oscillation with impacts on salmon production. Bull. Am. Meteorol. Soc. *78*, 1069–1079.

Mardia, K.V., Kent, J.T., and Bibby, J.M. (1979). Multivariate analysis (Academic Press).

Merkel, U., and Latif, M. (2002). A high resolution AGCM study of the El Nino impact on the North Atlantic/European sector. Geophys. Res. Lett. *29*, 5–1–5–4.

Nilson, E., Krahe, P., Lingemann, I., Horsten, T., Klein, B., Carmabia, M., and Larina, M. (2014). Auswirkungen des Klimawandels auf das Abflussgeschehen und die Binnenschifffahrt in Deutschland. KLIWAS-Schriftenreihe.

Petrow, T., and Merz, B. (2009). Trends in flood magnitude, frequency and seasonality in Germany in the period 1951–2002. J. Hydrol. *371*, 129–141.

Pozo-Vázquez, D., Esteban-Parra, M.J., Rodrigo, F.S., and Castro-Diez, Y. (2001). The association between ENSO and winter atmospheric circulation and temperature in the North Atlantic region. J. Clim. *14*, 3408–3420.

Rayner, N.A., Parker, D.E., Horton, E.B., Folland, C.K., Alexander, L.V., Rowell, D.P., Kent, E.C., and Kaplan, A. (2003). Global analyses of sea surface temperature, sea ice, and night marine air temperature since the late nineteenth century. J. Geophys. Res. Atmospheres 1984–2012 *108*.

Rimbu, N., Dima, M., Lohmann, G., and Musat, I. (2005). Seasonal prediction of Danube flow variability based on stable teleconnection with sea surface temperature. Geophys. Res. Lett. *32*.

Screen, J.A., and Simmonds, I. (2010). The central role of diminishing sea ice in recent Arctic temperature amplification. Nature *464*, 1334–1337.

Wallace, J.M., and Gutzler, D.S. (1981). Teleconnections in the geopotential height field during the Northern Hemisphere winter. Mon. Weather Rev. *109*, 784–812.

Winterscheid, A., Dietrich, S., Entelmann, I., and Ohle, N. (this issue). Implications of fresh-water discharge on estuarine sediment dynamics.

Zhou, S., Miller, A.J., Wang, J., and Angell, J.K. (2001). Trends of NAO and AO and their associations with stratospheric processes. Geophys. Res. Lett. *28*, 4107–4110.